Asian Journal of Chemistry; Vol. 32, No. 10 (2020), 2594-2600

ASIAN JOURNAL OF CHEMISTRY

https://doi.org/10.14233/ajchem.2020.22813

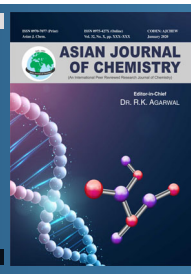

Complexes of Pyrimidine Thiones: Mechanochemical Synthesis and Biological Evaluation

POOJA SETHI[1,*], RAJSHREE KHARE[2] and RENUKA CHOUDHARY[3]

[1]Department of Chemistry, Maharishi Markandeshwar Deemed to be University, Mullana, Ambala-133207, India
[2]Principal, M.P.N. College, Mullana, Ambala-133207, India
[3]Department of Biotechnology, Maharishi Markandeshwar Deemed to be University, Mullana, Ambala-133207, India

*Corresponding author: E-mail: pooja.amb80@gmail.com

Received: 5 May 2020; *Accepted*: 7 July 2020; *Published online*: 25 September 2020; AJC-20075

A new series of metal complexes with 1-(2-methylphenyl)-4,4,6-trimethyl pyrimidine-2-thione (**2-HL1**) and 1-(4-methylphenyl)-4,4,6-trimethyl pyrimidine-2-thione (**4-HL2**) ligands, $[M(mppt)_2(H_2O)n]$ (M(II) = Cu, Mn, Co; n = 2 and M(II) = Ni, Zn; n = 0) have been synthesized using mechanochemical protocol. The complexes have been framed as $[M(mppt)_2(H_2O)n]$ due to 1:2 (metal:ligand) nature of these metal complexs. Structures have been further confirmed on the basis of elemental analysis, Magnetic susceptibility measurements, electronic, infrared, far infrared, proton NMR, Mass spectral moment and thermogravimetric analysis studies. The infrared spectral data suggested that ligand behaves as a bidentate, coordinating through – N (endocyclic) and – S (exocyclic) donor atoms. All the compounds have also been screened for antibacterial and DNA photocleavage potential. Ligands complexed with Mn and Ni metals have shown the effect of substitution on their biological potentials. It was found that substitution at 4th or *para* position makes the ligand and its metal complexes have better antibacterial and DNA photocleaving agents.

Keywords: DNA photocleavage, Pyrimidine-2-thione, Mechanochemical protocol.

INTRODUCTION

Pyrimidine-based heterocyclic thiones are regarded as privileged ligands [1] and metal complexes derived from these sulphur containing scaffolds have been known for decades. These complexes have been comprehensively studied due to their sensitivity, synthetic plasticity and selectivity towards a variety of metal atoms. Their importance in structural research as well as synthesis owes much to their derivative affluence and structural plurality. Pyrimidine-thione contains nitrogrn and sulphur donor atoms, the sulphur atom, is a soft center and the nitrogen atom is a hard center [2], this hard – soft combination allows to coordinate with the metals. There are various ways in which thione ligand approach metals, *via* sulphur bonding/sulphur bridging/N, S-chelating and N, S-bridging modes. The presence of –N(H)–C(=S)– moiety [3] is mainly responsible for the biological and pharmacological activity of pyrimidine-thiones. So the compounds having this moiety represent an important class of compounds as pharmaceutical and medicinal agents with a wide variety of pharmacological activity like antibacterial, antifungal, antileishmanial, anti-inflammatory, analgesic, antihypertensive, antipyretic, antiviral, antidiabetic, antiallergic, anticonvulsant, antioxidant, antihistaminic, herbicidal and anticancer activities [4-8].

In continuation of our research [9,10] to explore the potentialibility of some metal complexes compounds, it was planned to synthesize, mechanochemically pyrimidine-2-thione based metal complexes *viz.* $[Mn(2\text{-mppt})_2(H_2O)_2]\cdot H_2O$ (**1**), $[Mn(4\text{-mppt})_2(H_2O)_2]$ (**2**), $[Co(4\text{-mppt})_2(H_2O)_2]\cdot 4H_2O$ (**3**), $[Ni(2\text{-mppt})_2(H_2O)_2]\cdot 2.5H_2O$ (**4**), $[Ni(4\text{-mppt})_2(H_2O)_2]\cdot 2.5H_2O$ (**5**), $[Cu(4\text{-mppt})_2(H_2O)_2]$ (**6**) and $[Zn(2\text{-mppt})_2]\cdot H_2O$ (**7**). Furthermore, an effort has been made to find some new potential DNA photocleavage and antibacterial agents.

EXPERIMENTAL

All the chemicals used were of analytical grade and purchased from Hi-Media and used as such. The experimental work was carried out with double distilled water. The bacterial strains were isolated from the patients at M.M. Medical College, Maharishi Markandeshwar (Deemed to be University), Mullana, India. Plasmid DNA pUC 18 was used for accomplishing the photocleavage studies.

Physical measurements: The ^{1}H NMR spectra of the ligand and complexes were measured in DMSO-d_6 using TMS as reference standard on Bruker 400 MHz instrument. Q-ToF Micro Waters LC-MS spectrometer was used for the recording of the mass spectra. Elemental analyses (C, H, N) was carried out using LECO 9320 analyzer (Saif Lab, Chandigarh). IR, electronic and Mass spectra were measured on Shimadzu IR affinity in 4000 to 200 cm^{-1} range using KBr pellet method, Shimadzu UV 1800 instrument in DMSO as a solvent and on Agilent mass spectrometer.

Synthesis of ligands: The starting ligands 1-[2/4-methylphenyl]-4,4,6-trimethyl-3*H*,5*H*-dihydropyrimidine-2-thione (2/4-Hmppt) were synthesized according to reported literature method [11].

(2-Hmppt) (2-HL1): Off white, Yield: 64%; m.p. 199 °C. Anal. calcd. (found) % for $C_{14}H_{18}N_2S$: C, 67.2 (67.3); H, 7.3 (7.3); N, 11.3 (11.4); S, 13.0 (12.9).

(4-Hmppt) (4-HL1): Off white, Yield: 71%; m.p. 201 °C. Anal. calcd. (found) % for $C_{14}H_{18}N_2S$: C, 66.4 (66.6); H, 6.9 (7.0); N, 10.6 (10.7); S, 11.9 (12.1).

Synthesis of metal complexes: Mechanochemical method was employed to synthesize all metal complexes.

[Mn(2-mppt)$_2$(H$_2$O)$_2$]·H$_2$O (1): To solid ligand (**2-HL1**) (0.1 mol), solid Na salt (0.1 mol) was added, then it was grinded in a mortar with the help of a pestle for 1 h at room temperature and dried in sunlight for 2-3 days. Then $Mn(CH_3COO)_2{\cdot}4H_2O$ (0.05 mol) was added and again grinded for about 30 min and dried in air with occasional mixing in between). The product obtained was first washed with methanol then by petroleum ether to eliminate traces of unreacted metal salts. The complex obtained was coloured and stable at room temperature. Colour: light brown, Yield: 92%; m.p. 270 ºC. Elemental anal. calcd. (found) % for $C_{28}H_{40}N_4O_3S_2Mn$: C, 56.1 (55.8); H, 6.67 (5.5); N, 9.3 (9.0); S, 10.68 (10.4); O, 8.0 (7.7). IR (KBr, cm^{-1}): ω(O-H), 3391; ν(C=N) + (C=C), 1518; ν(NCS), 1407; ν(C=N) + ν(NCS) + ν(C=S), 1333, 1238, 1105; ν(C-S), 862; ω(Mn-N), 370; ω(Mn-S), 233. MS *m/z* [M+1]$^+$: 547.3.

[Mn(4-mppt)$_2$(H$_2$O)$_2$] (2): The same procedure was used as for complex **1** with **4-HL2** (0.1 mol). Light brown, Yield: 92% (based on $Mn(CH_3COO)_2{\cdot}4H_2O$. m.p. 272 °C. Elemental anal. (found) % for $C_{28}H_{38}N_4S_2O_2Mn$: C, 57.8 (56.8); H, 6.5 (6.1); N, 9.6 (8.4); S, 11.0 (10.6); O, 5.5 (5.1). IR (KBr, cm^{-1}): ν(O-H), 3440; ν(C=N) + ν(C=C), 1520; ν(NCS), 1406; ν(C=N) + ν(NCS) + ν(C=S), 1332, 1254, 1132; ν(C-S), 781, ν(Mn-N), 361; ν(Mn-S), 226. MS *m/z* [M+1]$^+$: 547.3.

[Co(4-mppt)$_2$(H$_2$O)$_2$]·4H$_2$O (3): The same reaction procedure was used as for complex **1** with **4-HL2** (0.1 mol) and $Co(CH_3COO)_2{\cdot}4H_2O$ (0.05 mol) respectively. Light violet, Yield: 85%; m.p. 308 ºC. Elemental anal. calcd. (found) % for $C_{28}H_{46}N_4S_2O_6Co$: C, 51.1 (50.1); H, 7.0 (6.4); N, 8.5 (8.0); S, 9.7 (8.9); O, 14.6 (14.2). IR (KBr, cm^{-1}): ν(O-H) 3448; ν(C=N) + ν(C=C),1521; ν(NCS), 1418; ν(C=N) + ν(NCS) + ν(C=S), 1333, 1238, 1105; ν(C-S), 717; ν(Co-N), 301; ν(Co-S) 210. MS *m/z* [M+1]$^+$: 550.7

[Ni(2-mppt)$_2$(H$_2$O)$_2$]·2.5H$_2$O (4): The same reaction procedure was used as for complex **1** with **4-HL2** (0.1 mol) and $Ni(CH_3COO)_2{\cdot}4H_2O$ (0.05 mol). Greenish, Yield: 91.8%; m.p. 328 °C. Elemental anal. calcd. (found) % for $C_{28}H_{43}N_4O_{4.5}S_2Ni$: C, 53.3 (53.0); H, 6.8 (5.9); N, 8.9 (8.4); S, 10.1 (9.7); O, 11.4 (11.0). IR (KBr, cm^{-1}): ν(O-H), 3407; ν(C=N) + ν(C=C), 1519; ν(NCS), 1406; ν(C=N) + ν(NCS) + ν(C=S), 1333, 1238, 1131; ν(C-S), 821; ν(Ni-N), 349; ν(Ni-S) 200. MS *m/z* [M+1]$^+$: 551.3.

[Ni(4-mppt)$_2$(H$_2$O)$_2$]·2.5H$_2$O (5): The same reaction procedure was used as for complex **1** with **4-HL2** (0.1 mol) and $Ni(CH_3COO)_2{\cdot}4H_2O$ (0.05 mol), respectively. Greenish, Yield: 91.8%. m.p. 328 ºC. Elemental anal. calcd. (found) % for $C_{28}H_{43}N_4O_{4.5}S_2Ni$: C, 53.3 (53.0); H, 6.8 (5.9); N, 8.9 (8.4); S, 10.1 (9.7); O, 11.4 (11.0). IR (KBr, cm^{-1}): ν(O-H), 3407; ν(C=N) + ν(C=C), 1518; ν(NCS), 1407; ν(C=N) + ν(NCS) + ν(C=S), 1333, 1238, 1105; ν(C-S), 821; ν(Ni-N), 350; ν(Ni-S) 279. MS *m/z* [M+1]$^+$: 551.3.

[Cu(4-mppt)$_2$(H$_2$O)$_2$] (6): The same reaction procedure was used as for **1**, with (**4-HL2**) (0.1 mol) and $Mn(CH_3COO)_2{\cdot}4H_2O$ was replaced by $Cu(CH_3COO)_2{\cdot}H_2O$ (0.05 mol). Light Green, Yield: 89% (based on $Co(CH_3COO)_2{\cdot}4H_2O$). m.p. 314 °C. Elemental anal. calcd. (found) % for $C_{28}H_{34}N_4O_2S_2Cu$: C, 57.0 (55.3); H, 6.4 (6.0); N, 9.5 (8.3); S, 10.8 (9.9); O, 5.4 (5.1). IR (KBr, cm^{-1}): ν(O-H), 3439; ν(C=N) + ν(C=C), 1507; ν(NCS), 1409; ν(C=N) + ν(NCS) + ν(C=S), 1333, 1308, 1103; ν(C-S), 819; ν(Cu-N), 284; ν(Cu-S) 174. MS *m/z* [M+1]$^+$: 555.2.

[Zn(2-mppt)$_2$]·H$_2$O (7): The same reaction procedure was used as for complex **1** with **4-HL1** (0.1 mol) and $Zn(CH_3COO)_2{\cdot}2H_2O$ (0.05 mol). White, Yield: 86.3% (based on $Zn(CH_3COO)_2{\cdot}2H_2O$). m.p. 313 ºC. Anal. calcd. (found) % for $C_{28}H_{36}N_4OS_2Zn$: C, 58.6 (57.2); H, 6.3 (6.1); N, 9.8 (8.9); S, 11.2 (10.4); O, 2.8 (2.4). IR (KBr, cm^{-1}): ν(O-H), 3280; ν(C=N) + ν(C=C), 1518; ν(NCS), 1408; ν(C=N) + ν(NCS) + ν(C=S), 1332, 1238, 1131; ν(C-S), 754; ν(Zn-N), 474; ν(Zn-S) 217. MS *m/z* [M+1]$^+$: 557.3.

Study on *in vitro* antibacterial activity: Antibacterial activities of synthesized compounds against various pathogenic strains of bacteria (*Bacillus subtilis* (5021), *S. aureus* (2063), *P. syringae* (5102), *P. aeruginosa* (5029)) were evaluated using agar well diffusion method. Plates containing 25 mL of nutrient agar were inoculated by swabbing 100 µL inocula of each test bacterium. Wells were bored after 15-20 min of adsoption of incula using sterile cork borer (10 mm diameter). At 2000 µg/L of concentration stock solutions of the standard and test compounds were prepared in DMSO. Two-fold dilution of the compounds (50 µL volume) from the stock solution (2, 4, 8,..1054 µg/mL) were inoculated into the corresponding wells in the seeded agar plates. Incubation of the innoculated plates were done at 37 °C for 24 h. Inhibition zone was evaluated for the detection of antibacterial activity of each synthesized compound with zone reader (Hi Antibiotic zone scale). DMSO was used as a negative control, where as oxacillin or penicillin G was used as a reference drug in the investigation.

DNA photocleavage studies: Agarose gel electrophoresis was used to study the DNA photocleavage activity by metal complexes. Firstly, metal complex (40 µg) was added with supercoiled plasmid DNA (5 µL) and incubated at 37 °C for 1 h. Later, Agarose (0.8%) gel was prepared and immersed into the electrophoresis tank containing 1X TAE buffer. DNA

samples were loaded into the wells by mixing with loading dye (0.25 % bromophenol blue, 0.25 % xylene cyanol, 30 % glycerol). After the electrophoresis at 90 V for 2 h, staining of the gel was done with ethidium bromide, (1.0 µg/mL) viewed under UV trans-illuminator (Bio-Rad UV trans-illuminator 2000).

RESULTS AND DISCUSSION

The synthesized ligands and their metal complexes were stable at room temperature and readily soluble in DMF/DMSO shown in **Scheme-I**. The mononegative bidentate ligand is probable to coordinate with metal centers *via* deprotonated cyclic nitrogen (N-3) and thione sulfur atoms (**Scheme-I**) which was confirmed using different spectroscopic techniques. We tried to structurally characterize one of the complex by X-ray crystallography, but unsuccessful to collect the data due to very slight crystal dimensions. All the complexes were characterized on the basis of ^{1}H NMR, IR, UV-visible spectroscopy, mass spectrometry, magnetic moment and thermogravimetric studies.

FTIR spectra: FTIR spectra was recorded in the region 4000-250 cm^{-1} and some specific bands and their assignments are listed in Table-1. In FTIR spectra, ν(N-H) stretching bands appeared at 3019 cm^{-1} in **2-HL1** and at 3028 cm^{-1} in **4-HL1**. The bands at 1691cm^{-1} in **2-HL1** and 1692 cm^{-1} in **4-HL1** respectively are due to δ(N-H) deformations [12,13]. Due to absence of any band for ν(SH) in 2600-2500 cm^{-1} region confirms the thione form of ligand [9,10,14].

After chelation, disappearance of ν(NH) stretching bands and advent of strong band in the range 1543-1510 cm^{-1} are assigned to the combination of ν(C=C) + ν(C=N) skeletal vibrations of pyrimidine-thione ring. These bands are shifted to low or high frequency signifying N-coordination occur through deprotonated ring nitrogen [15,16]. Besides, these in **2-HL1** bands at 1273, 1137 cm^{-1} and in **4-HL1** bands at 1276, 1136 cm^{-1} are allocated to contribution due to prevailing ν(C=S), which shows lower intensities or sometimes absence in the spectra of metal complexes. This specifies the association of exocyclic sulphur atom in coordination. Appearance of bands at or near 862-781 cm^{-1} due to C-S, further supports the participation of sulphur in coordination [12,13,17]. Due to extensive coupling

Step-I:

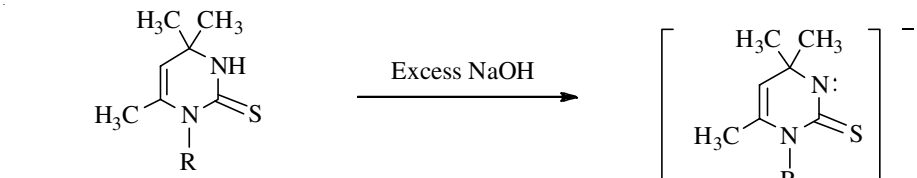

where R = *o*-$C_6H_4CH_3$, *p*-$C_6H_4CH_3$

Step-II:

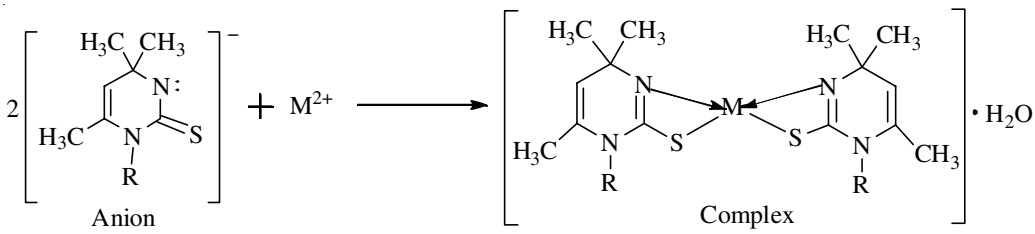

M^{2+} = Mn(II), Co(II), Ni(II), Cu(II), Zn(II)

Scheme-I

TABLE-1
FTIR DATA OF LIGANDS AND THEIR METAL COMPLEXES

Ligand/ complexes	Key IR bands (cm^{-1})								
	ν(OH)	ν(NH)	δ(NH)	ν(C=N) + ν(C=C)	ν(NCS)	ν(C=N) + ν(NCS) + (C=S)	ν(C–S)	ν(M–N)	ν(M–S)
Ligand									
2-HL1	–	3019	1691	1536	1495	1384, 1273, 1137	–	–	–
4-HL1	–	3028	1692	1508	1454	1385, 1276, 1136	–	–	–
Complexes									
1	3391	–	–	1518	1407	1333, 1238, 1105	862	370	233
2	3440	–	–	1520	1406	1332, 1254, 1132	781	361	226
3	3448	–	–	1521	1418	1333, 1238, 1105	717	301	210
4	3407	–	–	1519	1406	1333, 1238, 1131	821	349	200
5	3407	–	–	1518	1407	1333, 1238, 105	821	350	279
6	3439	–	–	1507	1409	1333, 1308, 1103	819	284	174
7	3280	–	–	1518	1408	1332, 1238, 1131	754	474	217

of δ(NH), ν(N-C=S), ν(C=N) and ν(C=S) called thioamide bands in the spectra of complexes infers that there is interaction between exocyclic S atom, ring N and metal ions [17,18].

Appearance of non-ligand bands in far IR spectra of complexes between 410 and 174 cm^{-1} are assigned to ν(M-N) and ν(M-S) stretches respectively [18-21]. It further confirms that N, S chelation takes place *via* the deprotonated nitrogen N-3 and the exocyclic sulphur atom [21,22].

^{1}H NMR spectra: ^{1}H NMR spectra of both ligands were documented in DMSO. The spectra of **2-HL1** exhibits singlets at δ 1.25, 1.33, 2.08, 4.94, 8.81 ppm which were allocated as 2(CH_3), 1(CH_3), 1(CH_3), C=C-H and N-H, respectively (Table-2). Multiplet of ArC-H appeared at δ 7.07-7.25 ppm. The spectrum of **4-HL1** exhibit singlet at δ 1.25, 1.40, 2.3, 4.91, 8.80 ppm, assigned as 2(CH_3), 1(CH_3), 1(CH_3), C=C-H and N-H respectively and the appearance of two doublet of doublet at δ 6.9-7.0(dd), 7.1-7.2(dd) ppm are due to ArC-H [19-25].

TABLE-2
^{1}H NMR (ppm) DATA OF **2-HL1**, **4-HL1** AND ITS METAL COMPLEXES

Protons	(2-HL1)	(4-HL1)	7
$4CH_3$	1.25,1.33,2.08	1.25,1.40,2.3	1.27-1.71
C=C-H	4.94	4.91	4.85
N-H	8.81	8.80	–
Ar-C-H	7.07-7.25	6.9-7.0 (dd) 7.1-7.2 (dd)	7.01-7.18

Absence of NMR signals at 8.81 ppm and 8.96 ppm for Nitrogen protons in the spectra of metal complexes further confirms the deprotonation of N-H and chelation of metal ion through the deprotonated N(3) [21]. Likewise, chemical shifting is observed in the values of all metal complexes as compared to free ligands. Broad peak appeared for NMR spectra of Cu, Ni and Mn complexes shows paramagnetic behaviour of the metal ions [26,27]. This statement is in full agreement with the reported results, which further approves the formation of metal complexes.

Mass spectra: The mass fragmentation of both ligands and selected metal complexes are reported in Table-3. The intense molecular ion peak appeared at *m/z* 247.52 (M^++1) in mass spectra of both ligands corresponds to its molecular formula (calcd. 246). Complex **1** exhibits a peak at *m/z* 547.35 corresponding to $[Mn(2\text{-mppt})_2]^+$ ion, while complex **5** shows a peak at *m/z* 551.32 due to $[Ni(4\text{-mppt})_2]^+$ ion. The mass spectrum of complex **6** shows a peak at *m/z* 555.29 corresponding to $[Cu(p\text{-mppt})_2]^+$ ion and the spectrum of complex **7** shows a peak at *m/z* 557.31 due to $[Zn(2\text{-mppt})_2]^+$ ion. Spectroscopic analysis provides sufficient proof to validate the formation of the expected metal complexes with the ligand in stoichiometric ratio of 1:2 (metal:ligand). This allows us to propose a *cis*-coordination geometry [9,25,28,29] for the metal complexes (**Scheme-I**).

Magnetic measurements and electronic spectra: The magnetic data of metal complexes are given in Table-4. The magnetic moment of metal complexes **1** and **2** shows value 5.68 and 5.66 BM, respectively which is expected for high spin distorted octahedral complexes [24]. Complex **3** shows magnetic moment of 3.67 BM and this value matches with values reported for octahedral complexes [30,31]. The magnetic data of complexes **4** and **5** show magnetic moment of 3.11 and 2.98 BM, which are close to that of an octahedral d^8 system with two unpaired electrons [32,33]. The value of 1.79 BM in complex **6** is due to one unpaired electron (S = ½) as mostly observed for copper complexes while Zn(II) have zero unpaired electron, shows diamagnetic behaviour [34].

TABLE-4
ELECTRONIC ABSORPTION AND MAGNETIC MOMENT DATA OF **2-HL1, 4-HL1** AND ITS METAL COMPLEXES

Ligand/ Complex	Magnetic moment (BM)	λ_{max} (nm)
2-HL1	–	292, 304
4-HL1	–	283, 319
1 and **2**	5.68 and 5.66 (both ocahedral)	285, 667
3	3.67 (Octahedral)	701, 624, 526, 465, 282
4 and **5**	3.11and 2.98 (both ocahedral)	723, 585, 510, 284
6	1.79 (ocahedral)	410, 403
7	Diamagnetic	631, 605, 287

UV visible spectra: Electronic spectra of complexes **1** and **2** show the *d-d* transitions of t_{2g}^3 e_g^2 are frail and spin forbidden, rarely visible in the concentrated solutions. A weak band at 667, 669 may be assigned to $^6A_{1g} \rightarrow {}^4T_{1g}$ (G) transitions [35]. Absorptions of 701, 624, 526, 465 nm were allotted to $^4T_{1g} \rightarrow {}^4T_{2g}$ (F), $^4T_{1g} \rightarrow {}^4T_{1g}$ (P), $^4T_{1g} \rightarrow {}^4A_{2g}$ (F) transitions for complexes 1, 2 and **3**, respectively [36].

For d^8 system electronic bands visible at 723, 585, 510 which are given to $^3A_2g \rightarrow {}^3T_2g$, $^3A_2g \rightarrow {}^3T_{1g}$ (F), $^3A_{2g} \rightarrow {}^3T_{1g}$ (P) and charge transfer (CT) transitions for complexes **4** and **5**. The electronic spectra for complex **6** shows a broad band at 702 nm which is assigned to $^2B_{1g} \rightarrow {}^2E_{2g}$ transitions [37]. Therefore, copper complex was proposed with an octahedral geometry [9,10]. Complex **7** displayed the bands at 631 and 605 nm assigned to $^1A_{1g} \rightarrow {}^1B_{1g}$ and $^1A_{1g} \rightarrow {}^1E_{2g}$ shows, respectively four coordinate square planar geometry for complex [38] (Table-4).

Thermal studies: Thermogravimetric studies showed stability and degradation behaviour of complexes **1**, **3**, **4**, **7**. The primary thermal analysis data is listed in Table-5. Loss of weight below 140 °C in some of the complex is due to dehydration and colour changes from light to dark [9,16]. TG curves

TABLE-3
MASS FRAGMENTATION DATA OF 2/4-Hmppt AND THEIR METAL COMPLEXES (M^+ + 1) MODE

2/4-Hmppt	1	4	6	7
121.07, 136.10, 188.57, 215.57, 247.51 *m/z*	188.5, 247.5, 269.4, 270.1, 491.4, 499.4, 515.4, 531.4, 547.3, 599.2 *m/z*	247.5, 269.4, 271.5, 515.4, 551.3, *m/z*	215.5, 247.5, 269.4, 270.4, 277, 315.5, 515.4, 555.2 *m/z*	215.5, 247.5, 269.4, 270.1, 515.4, 555.3, 557.3 *m/z*

TABLE-5
THERMOGRAVIMETRIC DATA OF METAL COMPLEXES

Compound	Decomposition stages and assignment	Temp. (°C)	Weight loss (%): Found (calcd.)
$[Mn(2\text{-mppt})_2(H_2O)_2]\cdot H_2O$ $[C_{28}H_{40}N_4MnO_3S_2]$ (**1**)	1) Lattice water (hydrated water)	0-80	2.9 (3.1)
	2) Coordinated water (inside coordination sphere)	80-153	5.09 (4.7)
	3) $C_7H_{10}N_2$ elimination	153-330	20.5 (20.3)
	4) C_7H_7S	330-500	15.1 (15.3)
	5) $C_{13}H_{17}N_2$ elimination	500-800	35.8 (35.6)
$[Co(4\text{-mppt})_2(H_2O)_2]\cdot 4H_2O$ $[C_{28}H_{46}N_4CoO_4S_2]$ (**3**)	1) 4 Lattice water (hydrated water)	0-100	9.7 (9.69)
	2) Coordinated water (inside coordination sphere)	100-228	5.53 (5.5)
	3) $C_7H_{11}N_2$ elimination	228-328	18.9 (18.8)
	4) C_7H_7S	328-500	14.15 (14.0)
	5) $C_{13}H_{16}N_2$ elimination	500-800	32.9 (33.0)
$[Ni(2\text{-mppt})_2(H_2O)_2]\cdot 2.5H_2O$ $[C_{28}H_{42.5}N_4NiO_{4.5}S_2]$ (**4**)	1) 2.5Lattice water (hydrated water)	0-80	3.0 (2.9)
	2) Coordinated water (inside coordination sphere)	80-170	6.0 (5.9)
	3) $C_6H_{10}N_2$ elimination	170-270	20.1 (20.0)
	4) $C_7H_{10}S$	270-375	15.1 (15.09)
	5) $C_{14}H_{17}N_2$ elimination	375-800	35.2 (35.3)
$[Zn(2\text{-mppt})_2]\cdot H_2O$ $[C_{28}H_{36}N_4ZnOS_2]$ (**7**)	1) Lattice water (hydrated water)	0-100	7.0 (7.1)
	2) $C_7H_{10}N_2$ elimination	100-273	19.8 (20.71)
	3) C_7H_7S	273-372	15.5 (15.37)
	4) $C_{13}H_{17}N_2$ elimination	372-700	31.4 (31.45)

*Calculated in parentheses

showed four stages of decomposition starting from the loss of hydrated water, coordinated water and decomposition of mppt$^-$ moiety, which is further due to the break-down of the weak hetero {HN-C(ph), HN-N(1) or N(1)-CS or S-N(3)} bonds [9,21].

Thermogram of complex **1** shows five stages of weight loss in 0-80 ºC, 80-153 ºC, 153-330 ºC, 330-500 ºC and 500-800 ºC temperature regions. These weight losses are correspond to the removal of one hydrated water molecule (calcd. 3.1%, found 2.9%), two coordinated water molecules (calcd. 4.7%, found 5.09%), $C_7H_{10}N_2$ moiety (calcd. 20.3%, found 20.5%), C_7H_7S moiety (calcd. 15.3%, found 15.1%), $C_{13}H_{16}N_2$ moiety (calcd. 35.6%, found 35.8%), respectively thereby leaving the mixture of MnO, MnS and MnC_2 [9,21].

For complex **3**, thermogravimetric studies showed five steps of decomposition in the 0-100 ºC, 100-228 ºC, 228-328 ºC, 328-500 ºC and 500-800 ºC, respectively. The weight loss reveals the removal of four lattice water molecule (calcd. 9.69%, found 9.7%), two coordinated water molecules (calcd. 5.5%, found 5.53%), $C_7H_{11}N_2$ moiety (calcd. 18.8%, found 18.9%), C_7H_7N moiety (calcd. 14.0%, found 14.15%), $C_{13}H_{16}N_2$ fragments (calcd. 33.0%, found 32.9%), respectively and CoO residue contaminated with sulfide and carbide left behind [9,21].

Thermogram of complex **4** shows five TG inflections from 0-70 ºC, 70-150 ºC, 150-270 ºC and 270-450 ºC, 450-800 ºC. Removal of 2.5 lattice water molecules (calcd. 2.9%, found 3.0%), two coordinated water molecules (calcd. 5.9%, found 6.0%), $C_6H_{10}N_2$ moiety (calcd. 20.0%, found 20.1%), C_7H_7S moiety (calcd. 15.09%, found 15.1%), $C_{14}H_{17}N_2$ fragments (calcd. 35.3%, found 35.2%), respectively reveals the successive weight loss and leaving contaminated mixture of NiO with carbide and sulfide [9,21].

Thermogram of complex **7** explains four TG weight losses which ranges from 0-100 °C, 100-273 °C, 273-372 °C and 372-700 °C. The first weight loss was endothermic, may be due to the release of one lattice water molecule (calcd. 7.1%, found 7.0%), then another due to $C_7H_{10}N_2$ moiety (calcd. 20.71%, found 19.8%) while third and fourth indicates the removal of C_7H_7N moiety (calcd. 15.37%, found 15.5%) and $C_{13}H_{17}N$ fragments (calcd. 31.45%, found 31.4%) leaving ZnO + ZnS + ZnC_2 residue [9,21].

Biological evaluation

Antibacterial activity of the metal complexes: On comparing the experimental data discovered that the **4-HL1** and its metal complexes are more active than the **2-HL1** and its metal complexes against all bacteria (Table-6). The data confirmed that this activity increases considerably on coordination/chelation. In addition to that on coordination polarity of the metal ion reduces primarily due to partial sharing of its positive charge with the donor groups [39,40] with in the chelate ring which in turn, leads to proliferation in the lipophilicity of metal chelates, to make it more permeable through the lipid layer [41] of microorganisms thus terminating them more violently. Once the compound come into the microbial cell, it confines the growth of bacteria by binding at the active site of enzymes, involved in various vital biochemical processes like proteins synthesis and cell respiration in the cell. In all the metal complexes active sites involve the formation of hydrogen bonds with imino group which further leads to snooping with the cell wall synthesis due to hydrogen bond formation the cytoplasmic membrane damages and the cell permeability may also be changed causing the cell death. Bioactivity order of complexes found was **3** > **6** > **5** > **7** > **2** > **4-HL1**. The higher activity of **3**, **6** and **5** complexes of **4-HL1** proposes that, on coordination the polarity of Co(II), Cu(II) and Ni(II) ion is abridged to a larger extent due to overlap of the ligand orbital and partial sharing of the positive charge of the cobalt, copper and nickel ions with donor groups. Consequently, Co(II), Cu(II) and Ni(II) ions are easily adsorbed on the surface of the cell

TABLE-6
in vitro ANTIBACTERIAL ACTIVITY OF
2-HL1, **4-HL1** AND ITS COMPLEXES

Compounds	Diameter of growth of zone inhibition (mm)			
	B. subtilis -5021	*S. aureus* -2063	*P. syringae* -5102	*P. aeruginosa* -5029
2-HL1	12	12	12	10
4-HL2	15	14	16	14
1	10	12	10	10
2	14	15	15	16
3	41	33	38	35
4	11	13	13	14
5	21	19	19	26
6	40	31	29	38
7	16	13	20	21
Penicillin G	35	31	38	37
Oxacillin	36	36	38	37

wall of microorganisms. These adsorbed ions interrupt the respiratory process of the cells and obstructs the synthesis of proteins. This, in turn, controls further growth [42] of the organisms.

DNA photocleavage study: The most threatening danger to the humans nowadays is cancer can be overcome by the discovery of chemical nuclease. Transition metal complexes possess good nuclease activities and are known to bind specifically with DNA [43]. The DNA photo cleavage study result were presented in Fig. 1. It was observed from the results that under the same experimental conditions metal complexes of **4-HL1** are relatively more active than **2-HL1** and complexes. Fig. 1 revealed that in complex **2** (20 μg/μL), both SC and NC form are visible, in complex **1** (60 μg/μL) only OC form is visible and complex **3**, show almost complete degradation of plasmid DNA suggesting the strong nuclease activity of these complexes (20 μg/μL). However, in complex **5** (40 μg/μL) and (20 μg/μL) respectively, there was complete change of super coiled plasmid DNA into open circular and nicked coiled form is also visible suggesting high DNA photo cleaving capacity in case of complex **5**. In case of complex **6**, there was almost complete degradation of plasmid DNA suggesting the strong nuclease activity of complex **6** (20 μg/μL).

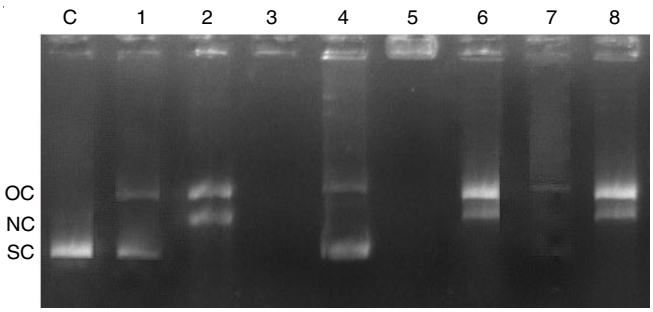

Fig. 1. DNA photocleavage activity of **2-HL1**, **4-HL1** and its complexes C control (DNA+DMSO), Lane 1-**4-HL1** (20 μg/μL), lane 2-complex **2** (20 μg/μL), lane 3- complex **3** (20μg/μL), lane 4-complex **5** (20 μg/μL), lane 5-complex **6** (40 μg/μL), lane 6-complex **6** (20 μg/μL), lane 7-**2-HL1** (60 μg/μL), lane 8-complex **4** (60 μg/μL)

In complex **4**, both the forms that is NC and OC were visible at 60 μg/μL. The better binding ability with plasmid DNA as compared to *ortho* substituted (2nd position) metal complexes leads to enhanced nuclease activity in case of *para* (4th position) substituted metal complexes and the different degree of binding ability of complexes with the plasmid DNA resulted difference in the nuclease activity among the *ortho* and *para* substituted metal complexes.

Conclusion

In search of some biologically active agents, some transition metal complexes of bidentate pyrimidine-2-thione were synthesized under mechanochemical conditions. Metal coordinate with ligand *via* endocyclic nitrogen and exocyclic sulphur thus forming a four membered ring. All of these compounds were evaluated for their DNA photocleavage ability and as antibacterial agents. It has been perceived that in comparison to ligand, its metal complexes **3**, **5** and **6** were found to reveal good DNA fragmentation and antibacterial potential. In future some structural alterations in the ligand may lead to formation of better DNA binding agents.

CONFLICT OF INTEREST

The authors declare that there is no conflict of interests regarding the publication of this article.

REFERENCES

1. K.M. Elattar, B.D. Mert, M. Monier and A. El-Mekabaty, *RSC Adv*., **10**, 15461 (2020); https://doi.org/10.1039/D0RA00411A
2. S.I. Mostafa, M.A. Kabil, E.M. Saad and A.A. El-Asmy, *J. Coord. Chem.*, **59**, 279 (2006); https://doi.org/10.1080/00958970500266149
3. E.S. Raper, *Coord. Chem. Rev.*, **153**, 199 (1996); https://doi.org/10.1016/0010-8545(95)01233-8
4. V. Sharma, N. Chitranshi and A.K. Agarwal, *Int. J. Med. Chem.*, **2014**, 202784 (2014); https://doi.org/10.1155/2014/202784
5. K.L. Haas and K.J. Franz, *Chem. Rev.*, **109**, 4921 (2009); https://doi.org/10.1021/cr900134a
6. M. Sonmez, M. Celebi, A. Levent, I. Berber and Z. Senturk, *J. Coord. Chem.*, **63**, 848 (2010); https://doi.org/10.1080/00958971003646506
7. G.M. Wu, W.L. Sun and Z.Q. Shen, *Chin. J. Polym. Sci.*, **27**, 293 (2009); https://doi.org/10.1142/S0256767909003923
8. T.S. Lobana, R. Sharma, G. Bawa and S. Khanna, *Coord. Chem. Rev.*, **253**, 977 (2009); https://doi.org/10.1016/j.ccr.2008.07.004
9. P. Sethi, P. Dogra, G.K. Gupta, S.I. Mostafa and S. Kaur, *Res. J. Chem. Environ.*, **22**, 73 (2018).
10. R. Khare and P. Sethi, *Int. J. Pharm. Pharm. Sci.*, **7**, 434 (2015).
11. R. Mathes, *J. Am. Chem. Soc.*, **75**, 1747 (1953); https://doi.org/10.1021/ja01103a519
12. K. Nakamoto, Infrared Spectra and Raman Spectra of Inorganic and Coordination Compounds, Part-B, Wiley: New York (1997).
13. M. Sonmez and M. Sekerci, *Synth. React. Inorg. Met.-Org. Chem.*, **33**, 1689 (2003); https://doi.org/10.1081/SIM-120025448
14. N.A. Lewis, F. Liu, L. Seymour, A. Magnusen, T.R. Erves, J.F. Arca, F.A. Beckford, R. Venkatraman, A. González-Sarrías, F.R. Fronczek, D.G. Van Derveer, N.P. Seeram, A. Liu, W.L. Jarrett and A.A. Holder, *Eur. J. Inorg. Chem*., **2012**, 664 (2012). https://doi.org/10.1002/ejic.201100898
15. S.I. Mostafa and F.A. Badria, *Met. Based Drugs*, **2008**, 723634 (2008); https://doi.org/10.1155/2008/723634
16. S. El-Sayed, B. Jean Claude, I. Butler and S. Mostafa, *J. Mol. Struct.*, **1028**, 208 (2012); https://doi.org/10.1016/j.molstruc.2012.05.073

17. A.K. Mishra, J. Jacob and K. Mullen, *Dyes Pigm*, **75**, 1 (2007); https://doi.org/10.1016/j.dyepig.2006.05.025
18. A.M. Ismail, W.M. Abou El Maaty, B.J. Jean-Claude and S.I. Mostafa, *Inorg. Chem. Commun.*, **106**, 217 (2019); https://doi.org/10.1016/j.inoche.2019.04.024
19. E. López-Torres and M.A. Mendiola, *Polyhedron*, **24**, 1435 (2005); https://doi.org/10.1016/j.poly.2005.03.093
20. G. Golub, H. Cohen, P. Paoletti, A. Bencini and D. Meyerstein, *J. Chem. Soc., Dalton Trans.*, **10**, 2055 (1996); https://doi.org/10.1039/DT9960002055
21. F.A. El-Morsy, B.J. Jean-Claude, I.S. Butler, S.A. El-Sayed and S.I. Mostafa, *Inorg. Chim. Acta*, **423**, 144 (2014); https://doi.org/10.1016/j.ica.2014.07.031
22. S.I. Mostafa, *Transition Met. Chem.*, **23**, 397 (1998); https://doi.org/10.1023/A:1006948815853
23 S.I. Mostafa, *J. Coord. Chem.*, **61**, 1553 (2008); https://doi.org/10.1080/00958970701598977
24. S.I. Mostafa, *Transition Met. Chem.*, **32**, 769 (2007); https://doi.org/10.1007/s11243-007-0247-x
25. A. Rodriguez, A. Sousa-Pedrares, J.A. Garcia-Vazquez, J. Romero and A. Sousa, *Eur. J. Inorg. Chem.*, 3403 (2011); https://doi.org/10.1002/ejic.201100156
26. B.A. Kim and H. So, *Bull. Korean Chem. Soc.*, **20**, 1145 (1999).
27. B.T. Thaker, K.R. Surati, P. Patel and S.D. Parmar, *J. Iran. Chem. Soc.*, **3**, 371 (2006); https://doi.org/10.1007/BF03245961
28. S. Roy, T.N. Mandal, A.K. Barik, S. Pal, S. Gupta, A. Hazra, R.J. Butcher, A.D. Hunter, M. Zeller and S.K. Kar, *Polyhedron*, **26**, 2603 (2007); https://doi.org/10.1016/j.poly.2007.01.006
29. A. Rodriguez, A. Sousa-Pedrares, J.A. Garcia-Vazquez, J. Romero and A. Sousa, *J. Organomet. Chem.*, **695**, 1271 (2010); https://doi.org/10.1016/j.jorganchem.2010.02.022
30. A.A.A. Emara and O.M.I. Adly, *Transition Met. Chem.*, **32**, 889 (2007); https://doi.org/10.1007/s11243-007-0245-z
31. J.R. Anacona, E. Bastardo and J. Camus, *Transition. Met. Chem.*, **24**, 478 (1999); https://doi.org/10.1023/A:1006997706762
32. J. Lewis and R.G. Wilkins, Modern Coordination Chemistry, Interscience: New York (1967).
33. M. Gulcan and M. Sonmez, *Phosphorus Sulfur Silicon Rel. Elem.*, **186**, 1962 (2011); https://doi.org/10.1080/10426507.2011.553501
34. B.N. Figgis, J. Lewis and F.A. Cotton, ed.: F.A. Cotton, Progress in Inorganic Chemistry, Interscience: New York (1964).
35. E.N. Sathyanarayana, Electronic Absorption Spectroscopy and Related Techniques, University Press: India (2001).
36. B.E. Douglas, D.H. McDaniel and J.J. Alexander, Concepts and Models of Inorganic Chemistry, Wiley: New York, edn 3 (1994).
37. L. Casella and M. Gullotti, *J. Am. Chem. Soc.*, **103**, 6338 (1981); https://doi.org/10.1021/ja00411a013
38. A.A. Osowole, R. Kempe, R. Schobert and K. Effenberger, *Synth. React. Inorg. Met. Org. Chem. Nano-Met. Chem.*, **41**, 825 (2011); https://doi.org/10.1080/15533174.2011.591310
39. Z.H. Chohan, A. Scozzafava and C.T. Supuran, *J. Enzyme Inhib. Med. Chem.*, **17**, 261 (2002); https://doi.org/10.1080/1475636021000006261
40. Z.H. Chohan, A. Scozzafava and C.T. Supuran, *J. Enzyme Inhib. Med. Chem.*, **18**, 259 (2003); https://doi.org/10.1080/1475636031000071817
41. U.M. Hassan, C.T. Chohan and C.T. Supuran, *Main Group Met. Chem.*, **25**, 291 (2002); https://doi.org/10.1515/MGMC.2002.25.5.291
42. Z.H. El-Wahab, M.M. Mashaly, A.A. Salman, B.A. El-Shetary and A.A. Faheim, *Spectrochim. Acta A Mol. Biomol. Spectrosc.*, **60**, 2861 (2004); https://doi.org/10.1016/j.saa.2004.01.021
43. Y. Liu, H. Chao, L. Tan, Y. Yuan, W. Wei and L. Ji, *J. Inorg. Biochem.*, **99**, 530 (2005); https://doi.org/10.1016/j.jinorgbio.2004.10.030